

Strong localization of photons in aperiodic optical waveguides: A numerical realization

Tsuneyoshi Nakayama, Kousuke Yakubo, and Motohiro Takano*

Department of Applied Physics, Hokkaido University, Sapporo 060, Japan

(Received 8 September 1992; revised manuscript received 7 December 1992)

Numerical demonstrations of the *strong* localization of light are presented by illustrating aperiodic two-dimensional waveguides. For this purpose, the correspondence between the discretized form of the wave equation for light and the vibrational equation of motion for lattice dynamics is discussed in a general form. We emphasize that this mapping is useful not only to gain insight into the nature of the strong localization of light, but also to perform large-scale simulations on this phenomenon by employing an accurate numerical technique. The results will serve as a useful guide for the modeling and design of optical waveguides in which one can observe the strong localization of light.

I. INTRODUCTION

The localization of light is currently of great interest, due to the possibilities for developing new frontiers of integrated optics and nonlinear optics.¹ The ultimate goal is the realization of the *strong* localization of light. Realistic modeling to observe such a phenomenon and the classification of its implication are most desirable. We discuss, in Sec. II of this paper, the corresponding relationship between the discretized form of the wave equation for light and the vibrational equation of motion for lattice dynamics. We emphasize that the correspondence is quite useful to gain insight into the design and modeling of systems to observe the strong localization of light. An additional merit of this mapping is that a powerful algorithm can be applied in order to numerically demonstrate the strong localization of light.^{2,3} This algorithm has been applied to problems of lattice dynamics of large and complex systems, and has also been successfully utilized in the mode analysis of optical waveguides.⁴

In Sec. III, we treat a simple optical waveguide that can be used to observe strongly localized light waves. Our system consists of a step-index optical waveguide with an aperiodic grating. Though our system is two dimensional (2D), it should be noted that the dimensionality does not play an important role for the *strong* localization phenomena of waves, in contrast with the case of weak localization. We present also, in Sec. III, our simulated results demonstrating that light is strongly localized in the optical waveguides with aperiodic gratings. Summary and discussions are given in Sec. IV.

II. LATTICE DYNAMICAL ASPECT OF THE WAVE EQUATION FOR LIGHT

The wave equation for electric fields \mathbf{E} , propagating in a medium with local refractive index $n(\mathbf{r})$, is⁵

$$\nabla^2 \mathbf{E} - \frac{n^2(\mathbf{r})}{c^2} \frac{\partial^2 \mathbf{E}}{\partial t^2} + \nabla \left[\frac{\nabla n^2(\mathbf{r})}{n^2(\mathbf{r})} \cdot \mathbf{E} \right] = 0, \quad (1)$$

where c represents the velocity of light in vacuum. Hereafter the system of units $c = 1$ is used. In general, Eq. (1)

can be reduced to the scalar wave equation for weakly guided systems by choosing a suitable polarization direction. This is, in fact, an excellent approximation for waveguides of practical interest.⁶ By setting the polarization to be in the x direction, Eq. (1) is reduced to

$$n^2(\mathbf{r})\psi_{tt}(\mathbf{r}, t) = \nabla^2 \psi(\mathbf{r}, t), \quad (2)$$

where the subscript tt means the second derivative with respect to time t , and $\psi(\mathbf{r}, t)$ represents electric fields of x direction at the spatial position \mathbf{r} . It should be emphasized that the third term of Eq. (1) vanishes exactly for electric fields \mathbf{E} propagating along the principal axis of step-index optical waveguides which are the main subject of this paper.

Discretizing the three-dimensional (3D) system by grids, the Laplacian in Eq. (2) can be written, for a lattice with grid spacings h_α along the α axis of Cartesian coordinates, in the form

$$n^2(ijk)\psi_{tt}(ijk) = - \sum_{\alpha} 2\psi(ijk)/h_{\alpha}^2 + \sum_{\alpha, e} \psi_{\alpha}^e(ijk)/h_{\alpha}^2, \quad (3)$$

where $\psi(ijk)$ is the value of the electric field at the grid point, $\mathbf{r} = (i, j, k)$. The symbol $\psi_{\alpha}^e(ijk)$ represents the electric field values at the nearest-neighbor points along the direction $e\alpha$ with $e = +$ and $-$ and $\alpha = x, y, \text{ and } z$.

One can relate Eq. (3) to the equation of a lattice vibration for scalar displacements. The corresponding equation of motion to Eq. (3) is described by

$$m(ijk)u_{tt}(ijk) = \sum_{lmn} K_{ijk}^{lmn} u(lmn), \quad (4)$$

where $m(ijk)$ and $u(ijk)$ are the mass and scalar displacement of the atom at the site (ijk) , respectively. The nondiagonal elements of K_{ijk}^{lmn} represent the Born-type force constant between atoms at (ijk) and (lmn) . The Born-type force constants K_{ijk}^{lmn} are nonzero for a nearest-neighbor interaction and zero otherwise. The diagonal elements must be chosen as

$$K_{ijk}^{ijk} = - \sum_{l \neq i, m \neq j, n \neq k} K_{ijk}^{lmn}$$

for a system which reflects the uniform-translational in-

variance of the system.⁷ Thus, we see that there is a correspondence between the discretized wave equation (3) and the vibrational equation of motion for lattice force constants $K_{ijk}^{i\pm 1, j, k} = 1/h_x^2$, $K_{ijk}^{i, j\pm 1, k} = 1/h_y^2$, and $K_{ijk}^{i, j, k\pm 1} = 1/h_z^2$ and diagonal elements $K_{ijk}^{ijk} = -(2/h_x^2) - (2/h_y^2) - (2/h_z^2)$. The squared refractive index $n^2(ijk)$ corresponds to mass $m(ijk)$ at the site (ijk) .⁹ The results obtained using this mapping seem, at first glance, to depend on the choice of the grid spacing h_α . However, this is not the case as described in Ref. 8.

The dynamical properties of random lattices have been extensively investigated both theoretically and numerically. It is well known that a random distribution of masses leads to the occurrence of localized modes. As a simple example, let us consider the situation where a single impurity with lighter mass (m) than that (M) of host atoms is embedded in a lattice. A localized mode appears at an eigenfrequency *above* the Debye cutoff frequency ω_D if the condition $m < 2M/3$ is satisfied for the 3D ($d=3$) case or $m < M$ for 1D.¹⁰ The localization becomes strong with increasing ratio between M and m . However, some caution is needed for the prediction of the strong localization of photons from the analogy between Eqs. (3) and (4) since the optical system is spatially continuous and the cutoff frequency ω_D should be *infinity*. The isolated domain of refractive index (mass) is irrelevant to the *strong* localization of light, even for the case of small refractive index domain (mass). This is because the spectral density of states (DOS) spreads over the infinite range ($\omega_D \rightarrow \infty$) and the corresponding eigenfrequencies are embedded in the continuous frequency band of the DOS, namely, the localized modes couple with the modes of continuous spectrum. Note that this type of disorder leads to the occurrence of *weakly* localized light. One has to introduce the ‘‘cutoff’’ frequency such as the case of lattice dynamics, i.e., a frequency gap is necessary in the DOS for the optical system to obtain the strong localization of light.¹¹

To design the optical system for our purpose, first the frequency gap in the DOS is necessary by taking into account the periodic structure of refractive index,^{11,13–16} and second we introduce the midgap states, in which the strongly localized modes are expected, by violating the periodic structure of refractive index. The accurate calculation of the DOS for the system is *crucial* for predicting the frequency region to observe the *strong* localization of light. We need, of course, to perform large-scale numerical simulations to demonstrate the strong localization of light.

III. MODEL PROPOSAL AND ITS SIMULATED RESULTS

In this section, we present the simulated results of the strong localization of light for our proposed system. Our system is illustrated in Fig. 1 with the definitions of coordinates. The active layer has a heterostructure in which two regions with different refractive indices (n_A, n_B) are alternately aligned. The active layer is surrounded by cladding layers with the refractive index n_C . We deal with electric fields in the y - z plane neglecting the x -axis

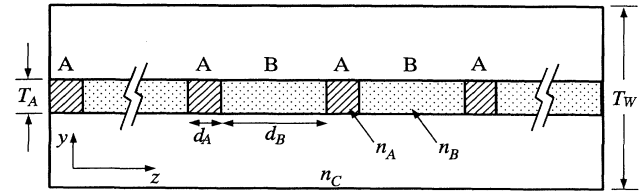


FIG. 1. The waveguide with aperiodic grating and the definitions of parameters. Active layer consists of the grating with two different refractive indices n_A and n_B .

dependence. This assumption does not seriously influence our main results.

The parameters used for our system, illustrated in Fig. 1, are the refractive indices (n_A, n_B, n_C), the thickness of the active layer (T_A), and that of the waveguide (T_W). The random distribution of refractive indices in the active layer is required to localize light waves. We have introduced aperiodicity in the active layer as follows: the length of the region A (or B) in the active layer is chosen as $d_A + x$ (or $d_B + x$), where x is a random variable under the condition $|x| \leq \alpha$. The positive parameter α represents the strength of disorder, i.e., periodicity is destroyed with increasing the value of α . To obtain strong localization, the mean free path l of light should be comparable to the wavelength. Short-range disorder (even strong), on length scales shorter than the wavelength, does not lead to the strong localization because of its averaging-out effect. The only way is to require the correlation length of disorder comparable to the wavelength of light. This point will be discussed later.

The grid spacings h_y and h_z must be taken small enough that amplitudes become sufficiently smooth on a scale of the grid spacing. This indicates that the numbers of grids (N_y and N_z) should be taken to be large enough. In our simulation, the thickness of the waveguide is taken as $T_W = 1 \mu\text{m}$ and that of the active layer as $T_A = 0.2 \mu\text{m}$. The total length of the waveguide is set to be $L_W = 36 \mu\text{m}$. We have taken grid spacings along the z and y axes as $h_z = 100 \text{ \AA}$ and $h_y = 200 \text{ \AA}$, respectively. The refractive indices are assumed to be $n_A = 2.5$, $n_B = 2.0$, and $n_C = 1.5$ (Note that the case of $n_C = 1$ corresponds to the isolated active layer such as the case fabricated by Jewell *et al.*¹²). The fundamental lengths of the regions A and B are taken to be $d_A = 900 \text{ \AA}$ and $d_B = 2700 \text{ \AA}$, respectively. Our system has 100 steps of index distribution along the z axis.

The accurate calculation of the spectral density of states (DOS) is crucial to pick up the localized eigenmodes of light waves, especially in the frequency region of the pseudogap. We show first the calculated results of the DOS's for the system without cladding layers. These results will clear up the difference between the cases *with* and *without* cladding layers.

At first, we show in Fig. 2(a) the calculated DOS for the case $\alpha = 0$ *without* cladding layers, in which the periodic boundary condition is applied in the z direction and the fixed boundary condition in the y direction.¹⁷ The first sharp peak close to $\nu = 315 \text{ THz}$ can be attribut-

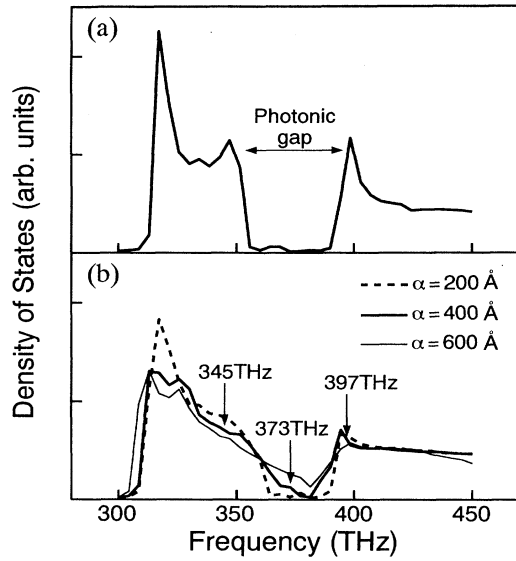


FIG. 2. The calculated DOS for (a) periodic and (b) aperiodic grating *without* cladding layers. The definition of the parameters are given in the text. The eigenmodes, belonging to the eigenfrequencies pointed by the arrows in the figure, are shown in Fig. 3.

ed to the mode with the set of wavelengths $\lambda_z = \infty$ and $\lambda_y = 2T_A$, which is the lowest eigenfrequency in our system. The origin of this sharp peak is due to the fact we have taken the fixed boundary condition at the edge of the waveguide. The frequency region between $\nu = 351$ and 396 THz corresponds to the lowest band gap. Figure 2(b) shows the calculated results of the DOS's for the case with random distribution of refractive indices in the active layer. We can realize, from the results of Fig. 2(b), that the photonic band gap between 351 and 396 THz is rounded off with increasing α , i.e., increasing degree of disorder.

Next, we have calculated in Fig. 3 the spatial distribution of squared amplitudes $|\psi(y,z)|^2$ for the case $\alpha = 400$ Å without claddings, belonging to eigenfrequencies (a) $\nu = 345$ THz, (b) 373 THz, and (c) 397 THz. The localization length has been calculated from the following relation:

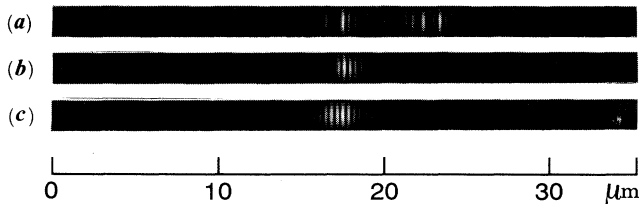


FIG. 3. The spatial distribution of squared amplitudes $|\psi(y,z)|^2$ for the case $\alpha = 400$ Å. The case (a) corresponds to the eigenmode with the eigenfrequency $\nu = 345$ THz, the case (b) corresponds to that of $\nu = 373$ THz, and the case (c) corresponds to that of $\nu = 397$ THz. The length scale is given on bottom.

$$\Lambda_z = \frac{\int |\mathbf{r}_z - \mathbf{r}_0| |\psi(y_c, z)| dz}{\int |\psi(y_c, z)| dz}. \quad (5)$$

Here the center of mode \mathbf{r}_0 is defined by

$$\mathbf{r}_0 = \frac{\int \mathbf{r}_z |\psi(y_c, z)| dz}{\int |\psi(y_c, z)| dz}, \quad (6)$$

where \mathbf{r}_z is the distance from an arbitrary point along the center line of the waveguide ($y = y_c$). If the amplitude follows the relation

$$|\psi(y_c, z)| = \psi_0 \exp(-|\mathbf{r}_z - \mathbf{r}_0|/\xi),$$

the characteristic length Λ_z defined in Eq. (5) becomes the localization length ξ . The localization lengths of these three modes have been obtained as (a) $3.17 \mu\text{m}$, (b) $0.73 \mu\text{m}$, and (c) $2.22 \mu\text{m}$, respectively. We see that the midgap state ($\nu = 373$ THz) in the pseudogap is most strongly localized. Thus, the accurate calculation of the DOS is crucial, especially the frequency region of the pseudogap, to pick up *strongly* localized modes of light.

We have performed the same calculations for the more realistic system *with* cladding layers. Figure 4 shows the calculated results of the DOS for $\alpha = 0$ (solid line) and $\alpha = 600$ Å (dotted line). The frequency region between 230 and 251 THz corresponds to the lowest photonic band gap for our system. It should be emphasized here, from the results of Fig. 4, that the pseudogap is appreciably rounded off even for the periodic case. This is because the system *with* cladding layers has a large translationally symmetric region (cladding), i.e., a lot of modes excited in the cladding layers contribute to the DOS, and the pseudogap arising from the periodic active layer is averaged out.

We have calculated the eigenmode belonging to the eigenfrequency 245 THz (the midgap state) for the case of $\alpha = 600$ Å. This is shown in Fig. 5, from which we can

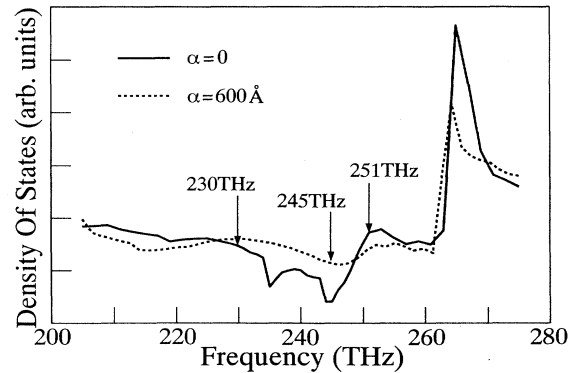


FIG. 4. The calculated DOS with cladding layers. The result of the solid line indicates the photonic pseudogap which appears between 230 and 251 THz. The dotted line shows the DOS for the case with aperiodic grating $\alpha = 600$ Å.

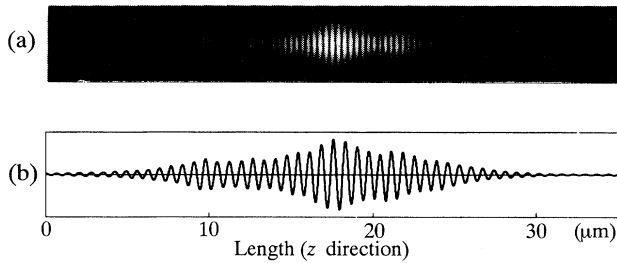


FIG. 5. (a) The calculated eigenmode for the case $\alpha=600 \text{ \AA}$ near the midgap state ($\nu=245 \text{ THz}$). The light waves are smearing out from the active layer into the cladding layers. The amplitude of electric fields is normalized as the case of Fig. 5. (b) The cross section of the amplitude of the same localized mode is plotted along the center line ($y=y_c$) of the active layer.

appreciate that this eigenmode is surely strongly localized. The localization length of this eigenmode is $\Lambda_z=4.59 \mu\text{m}$, which is larger than its wavelength $\lambda_z=2(d_A+d_B)=0.72 \mu\text{m}$. Note here that the localization length of the midgap state $\Lambda_z=0.73 \mu\text{m}$ for the case *without* cladding layers (shown in Fig. 3) is much shorter than the case of Fig. 5. This clear difference between the cases *with* and *without* cladding layers is interpreted as follows: the tails of localized waves smear out appreciably into the cladding layers as seen from the result of Fig. 5. This smearing-out effect prevents strong localization of light.

IV. SUMMARY AND DISCUSSION

In this paper, it has been demonstrated by computer simulations that the strong localization of light occurs for the realistic systems, namely, the optical waveguides with aperiodic grating. In Sec. II, we have discussed the corresponding relationship between the discretized form of the wave equation for light and the vibrational equation of motion for lattice dynamics. The mapping has the following advantages: (i) it is useful to gain insight into the strong localization of light from the analogy with lattice vibrations and (ii) we can employ an accurate numerical algorithm to perform large-scale numerical simulations for the present problem, which has been successfully applied to the problem of lattice dynamics of large and complex systems.

The numerical method^{2,3} employed in this paper is based on mechanical resonance to extract eigenmodes, and can deal with matrices of the size $10^6 \times 10^6$ for implementation on an array-processing supercomputer with 64 MB memory space. This algorithm has enabled us to accurately calculate the spectral density of states. We have proposed a system in which the strong localization of light is observed, which is actually obtainable by applying microfabrication techniques. We conclude that our results should serve as a useful guide for the design and modeling of the system to observe the strong localization of light.

ACKNOWLEDGMENT

This work was supported in part by a program of the Japan Ministry Education, Science and Culture.

*Present address: CSK Co. Ltd., Shinjuku-ku, Nishi-Shinjuku 2-6-1, Tokyo 163, Japan.

¹For reviews, see for example, A. Legendijk and M. P. van Albeda, *Phys. World* **3**, 33 (January 1990); S. John, *Phys. Today* **44**, 32 (May 1991).

²M. L. Williams and H. J. Maris, *Phys. Rev. B* **31**, 4508 (1985).

³K. Yakubo, T. Nakayama, and H. J. Maris, *J. Phys. Soc. Jpn.* **60**, 3249 (1991).

⁴For example, see K. Yakubo and T. Nakayama, *Phys. Rev. B* **40**, 517 (1989); K. Yakubo, E. Courtens, and T. Nakayama, *ibid.* **42**, 1078 (1990); T. Nakayama, M. Takano, K. Yakubo, and T. Yamanaka, *Opt. Lett.* **17**, 326 (1992).

⁵For example, see M. Born and E. Wolf, *Principles of Optics*, 6th ed. (Pergamon, Oxford, 1980), p. 10.

⁶See, for example, D. Marcuse, *Theory of Dielectric Optical Waveguides* (Academic, New York, 1991).

⁷It should be noted that the force constants K_{ijk}^{lmn} have a different sign from the definition of the dynamical matrix elements Φ_{ijk}^{lmn} normally used in the field of lattice dynamics. See M. Born and K. Huang, *Dynamical Theory of Crystal Lattices* (Clarendon, Oxford, 1954), Chap. IV.

⁸To clear up this point, consider an isotropic 2D rectangular sheet with the size $H_x \times H_y$, which is discretized by the $N_x \times N_y$ lattice ($N_x \times N_y$ are integers). For this case, the grid spacings h_x and h_y are determined through the relation $H_x = N_x h_x$ and $H_y = N_y h_y = N_y h_x \epsilon$ where $\epsilon = h_y/h_x$. Since a grid point \mathbf{r} on the sheet is represented by a set of integers (ij), one can set $h_x = 1$ and $h_y = \epsilon$ in Fig. 3 (Length scales are

measured in unit of $h_x = 1$). Namely, one can see that, if an anisotropic unit $h_x \times h_y$ is chosen, the force constant should be taken as $K_{ij}^{i\pm 1, j} = 1$ and $K_{ij}^{i, j\pm 1} = (1/\epsilon)^2$ without violating the step-size invariance.

⁹This correspondence is not unique for the mode-analysis of optical waveguides. In the case of the analysis presented in Ref. 5, the time development is replaced by the z axis along which the system has translational invariance.

¹⁰See, for examples, A. A. Maradudin, E. W. Montroll, and G. H. Weiss, in *Solid State Physics Supplement 3*, edited by F. Seitz and D. Turnbull (Academic, New York, 1963), Chap. 5, and J. Hori, *Spectral Properties of Disordered Chains and Lattices* (Pergamon, London, 1972).

¹¹S. John, *Phys. Rev. Lett.* **53**, 2169 (1984).

¹²J. L. Jewell, J. P. Harbison, A. Scherer, Y. H. Lee, and L. T. Floreg, *IEEE J. Quantum Electron.* **QE-27**, 1322 (1984).

¹³E. Yablonovitch and T. J. Gmitter, *Phys. Rev. Lett.* **63**, 1950 (1989).

¹⁴Z. Zhang and S. Satpathy, *Phys. Rev. Lett.* **65**, 2650 (1990).

¹⁵K. M. Ho, C. T. Chan, and C. M. Soukoulis, *Phys. Rev. Lett.* **65**, 3152 (1990).

¹⁶C. T. Chan, K. M. Ho, and C. M. Soukoulis, *Europhys. Lett.* **16**, 563 (1991).

¹⁷This boundary condition is not realistic for an actual situation. In addition, if the system is not isolated by metal coating, the localized states couple with the modes of continuous spectrum from the outside world.

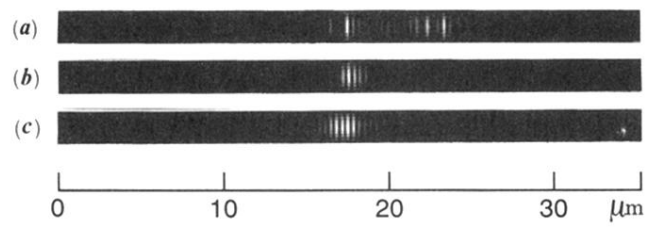


FIG. 3. The spatial distribution of squared amplitudes $|\psi(y,z)|^2$ for the case $\alpha=400 \text{ \AA}$. The case (a) corresponds to the eigenmode with the eigenfrequency $\nu=345 \text{ THz}$, the case (b) corresponds to that of $\nu=373 \text{ THz}$, and the case (c) corresponds to that of $\nu=397 \text{ THz}$. The length scale is given on bottom.

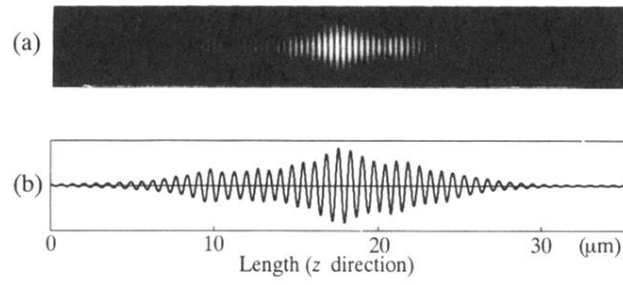


FIG. 5. (a) The calculated eigenmode for the case $\alpha = 600 \text{ \AA}$ near the midgap state ($\nu = 245 \text{ THz}$). The light waves are smearing out from the active layer into the cladding layers. The amplitude of electric fields is normalized as the case of Fig. 5. (b) The cross section of the amplitude of the same localized mode is plotted along the center line ($y = y_c$) of the active layer.